

1 **The limited spatial scale of dispersal in soil arthropods revealed with**
2 **whole-community haplotype-level metabarcoding**

3 Paula Arribas^{1,2,3}, Carmelo Andújar^{1,2,3}, Antonia Salces-Castellano¹, Brent C.

4 Emerson¹ & Alfried P. Vogler^{2,3}

5
6 ¹*Island Ecology and Evolution Research Group (IPNA-CSIC), Astrofísico Fco. Sánchez*
7 ³, 38206 La Laguna, Tenerife, Spain.

8 ²*Department of Life Sciences, Natural History Museum, Cromwell Road, London SW7*
9 ⁵BD, UK.

10 ³*Department of Life Sciences, Imperial College London, Silwood Park Campus, Ascot*
11 ^{SL5} 7PY, UK.

12 *Corresponding author: Paula Arribas, pauarribas@ipna.csic.es.*

13
14 **RUNNING TITLE:** Limited scale of dispersal in soil mesofauna

15
16 **ABSTRACT**

17 Soil arthropod communities are highly diverse and critical for ecosystem functioning.
18 However, our knowledge of spatial structure and the underlying processes of community
19 assembly is scarce, hampered by limited empirical data on species diversity and
20 turnover. We implement a high-throughput-sequencing approach to generate
21 comparative data for thousands of arthropods at three hierarchical levels: genetic,
22 species and supra-specific lineages. A joint analysis of the spatial arrangement across
23 these levels can reveal the predominant processes driving the variation in biological
24 assemblages at the local scale. This multi-hierarchical approach was performed using
25 haplotype-level-COI metabarcoding of entire communities of mites, springtails and

26 beetles from three Iberian mountain regions. Tens of thousands of specimens were
27 extracted from deep and superficial soil layers and produced comparative
28 phylogeographic data for >1000 co-distributed species and nearly 3000 haplotypes.
29 Local assemblage composition differed greatly between grasslands and forests, and
30 within each habitat showed strong spatial structure and high endemism. Distance-
31 decay was high at all levels, even at the scale of a few kilometres or less. The local
32 distance-decay patterns were self-similar for the haplotypes and higher hierarchical
33 entities, and this fractal structure was similar in all regions, suggesting that uniform
34 processes of limited dispersal determine local-scale community assembly. Our results
35 from whole-community metabarcoding provide insight into how dispersal limitations
36 constrain mesofauna community structure within local spatial settings over evolutionary
37 timescales. If generalized across wider areas, the high turnover and endemism in the
38 soil locally may indicate extremely high richness globally, challenging our
39 current estimations of total arthropod-diversity on Earth.

40

41

42 **KEYWORDS:** cMBC, dispersal, distance-decay, endemism, haplotype, soil
43 mesofauna, speciation scale.

44

45

46 INTRODUCTION

47 Soils are among the most biodiverse habitats on Earth, but represent probably the least
48 well studied, and thus poorly understood, terrestrial ecosystem (Bardgett & van der
49 Putten, 2014; Decaëns, 2010). Current understanding of terrestrial biodiversity has
50 mainly relied on studies of aboveground organisms, but in recent years these efforts have
51 been expanded towards the biodiversity of the soil (Thakur et al., 2019). However,
52 current knowledge is strongly unbalanced across taxonomic groups (Cameron et al.,
53 2018), which hampers the development of an integrative framework for understanding
54 the patterns and underlying mechanisms of soil biodiversity. In particular, there is a
55 pronounced shortage of basic data on species diversity and spatial structure for the
56 taxonomically and functionally diverse soil arthropods. They make up a large proportion
57 of the soil mesofauna composed of small-bodied invertebrates measuring between 0.1 –
58 2 mm and are found by the thousands in virtually every square meter of natural
59 soil (Bardgett, Usher, & Hopkins, 2005; Decaëns, 2010). Conventional taxonomic
60 approaches have been onerous, given the small body size, limited morphological
61 variation and high local abundances of most mesofauna components. High-throughput
62 sequencing so far has been applied mostly to microbial components of soil ecosystems
63 (e.g. Delgado-Baquerizo et al., 2018; Ramirez et al., 2018, 2014) while the study of soil
64 arthropod mesofauna has seen comparatively little progress in exploiting these tools
65 (mostly using 18S eDNA approaches Wu, Ayres, Bardgett, Wall, & Garey, 2011;
66 Zinger et al., 2019).

67 Existing work on the diversity, distribution and community composition of soil
68 arthropods has focussed on springtails and oribatid mites, and mostly has pointed to
69 selection by abiotic and/or biotic environmental factors as major mechanisms of
70 community assembly at the local scale (e.g. Caruso, Trokhymets, Bargagli, & Convey,

71 2013; Magilton, Maraun, Emmerson, & Caruso, 2019; reviewed in Berg, 2012; Thakur
72 et al., 2019). Different studies have also reported purely spatial structures (independent of
73 the measured environmental variables) or stochastic patterns (non-environmental neither
74 spatial structures) for the soil mesofauna communities, that have been
75 recurrently attributed to the contribution of demographic processes (i.e., ecological drift
76 without dispersal limitation) in determining the local community assembly (Bahram,
77 Kohout, Anslan, Harend, & Abarenkov, 2016; Ingimarsdóttir et al., 2012; Widenfalk,
78 Malmström, Berg, & Bengtsson, 2016; Zinger et al., 2019). In addition, dispersal
79 limitations have also been suggested to contribute to some of the spatial community
80 structures reported (Caruso, Taormina, & Migliorini, 2012; Gao, He, Zhang, Liu, & Wu,
81 2014). However, dispersal limitation still is rarely recognised as an important
82 mechanism of assembly of the soil mesofauna at the local scale (Berg, 2012; Thakur et
83 al., 2019). Beyond the aggregated distribution within the geographic ranges of the
84 species, limitations to dispersal can determine the degree to which species pools are
85 differentiated over spatial distance (Hortal, Roura-Pascual, Sanders, & Rahbek, 2010).
86 These effects are frequently evident as biogeographic or phylogeographic breaks at
87 large (regional to continent-wide) scales reflecting long-term population separation.
88 Similar patterns of species and haplotype turnover can arise even over relatively small
89 distances if the scale of movement is highly constrained and if the constraints are
90 persistent through time, as could be the case in the soil matrix. The potentially low
91 taxonomic resolution (due to morphological species assignment or the use of 18S rRNA
92 gene) of most of the studies on arthropod mesofauna communities may have missed the
93 importance of dispersal limitation in determining the diversity patterns of soil
94 mesofauna (but see Andújar et al., 2015; Lindo & Winchester, 2009).

95 The spatial scale at which dispersal constraints are effective in determining
96 species distributions and community assembly is a major “open question” in soil
97 biodiversity research (Thakur et al., 2019). For the mesofauna, small body size and high
98 local abundance may increase the probability of passive dispersal and long-distance
99 movement, and therefore dispersal constraints within the soil may be of limited
100 importance. High prevalence of aerial, aquatic and marine rafting has been
101 demonstrated for various mesofaunal lineages (Coulson, Hodkinson, Webb, & Harrison,
102 2002; Nkem et al., 2006; Schuppenhauer, Lehmitz, & Xylander, 2019), and studies have
103 shown mesofaunal assemblages with no apparent dispersal limitation across continental-
104 scale areas (Baird, Leihy, Scheepers, & Chown, 2019), especially for the smallest-
105 bodied soil arthropods (Gan, Zak, & Hunter, 2019). On the other hand, molecular
106 studies have revealed high differentiation and ancient microendemism even in
107 morphologically indistinguishable clades, indicating long-term constraints to
108 dispersal (Andújar, Pérez-González, et al., 2017; Cicconardi, Fanciulli, & Emerson,
109 2013). These empirical data limited to particular mesofauna lineages and their
110 contrasting findings highlight the difficulty of establishing the role of dispersal
111 constraints in community assembly. As such, inferences regarding the distribution and
112 diversification of edaphic species, and thus generalisations regarding macroecological
113 and macroevolutionary patterns, remain challenging.

114 New approaches to the study of diverse and cryptic arthropods using whole-
115 community metabarcoding (cMBC) using the mitochondrial COI gene are now
116 revolutionizing the understanding of complex arthropod communities (Arribas et al.,
117 2016; Ji et al., 2013). The methodology involves the bulk sequencing of mixed
118 communities and subsequent clustering of DNA reads into operational taxonomic units
119 (OTUs) that broadly represent the species category. While an efficient method to

120 approximate community profiles at the species-level, precise removal of primary DNA
121 reads affected by sequencing errors (Andújar, Arribas, Yu, Vogler, & Emerson, 2018;
122 Elbrecht, Vamos, Steinke, & Leese, 2018; Turon, Antich, Palacín, Præbel, &
123 Wangensteen, 2019) and co-amplified nuclear mitochondrial copies (numts) (Andújar et
124 al., 2020) would avert the need for clustering. Read-based data raise the prospect of
125 reliable haplotype information from mitochondrial COIcMBC, which represents a step
126 change for the study of diversity patterns through whole-community genetic analyses at
127 haplotype-level resolution.

128 Haplotype data can be used directly for analyses of genetic diversity, or after
129 aggregation into species-level entities for analyses of species diversity, which permits the
130 joint analysis of turnover (beta diversity) at multiple hierarchical levels. This approach
131 has been exploited to determine whether the composition in biological assemblages is
132 predominantly driven by dispersal or niche-based processes (Baselga et al., 2013;
133 Baselga, Gómez-Rodríguez, & Vogler, 2015). Local assemblages may diverge simply
134 due to the lack of population movement which, when assessed for entire
135 communities, results in a largely regular decay of community similarity with spatial
136 distance for the typically neutral haplotype variation of the mitochondrial COI gene.
137 Under a scenario where dispersal constraints determine the spatial community structure,
138 assemblage turnover at the species level should mirror these haplotype patterns, albeit at
139 a higher level of similarity. In contrast, niche-based processes acting on species traits
140 produce species distributions that mainly follow environmental factors and thus differ
141 from neutral conditions determining the haplotype distributions. This confounds the
142 correlation (self-similarity) of distance decay at the species and haplotype levels, as each
143 is driven by different processes. The self-similarity of distance decay of communities at
144 genetic and species levels therefore provides a formal test to discern if a particular

145 spatial pattern of community assemblage is predominantly driven by stochastic
146 dispersal or niche based processes, as the latter will not usually produce this
147 correlation (Baselga et al., 2013, 2015). In addition, multi-hierarchical analyses may also
148 describe the spatial scale at which dispersal constraints act, and the variation of scale
149 among different taxonomic groups or habitats (Gómez-Rodríguez, Miller, Castillejo,
150 Iglesias-Piñeiro, & Baselga, 2018; Múrria et al., 2017) . This framework remains to be
151 exploited with whole-community metabarcoding.

152 Here we apply the multi-hierarchical framework to study the spatial structure of
153 entire assemblages of mites (Acari), springtails (Collembola) and beetles (Coleoptera)
154 including many thousands of specimens, in a semi-natural mosaic landscape within
155 three geographically distinct mountain regions in southern and central Iberia (Fig. 1 A).
156 Our aim was to generate rigorous whole-community data at haplotype, putative species
157 (OTU) and supra-specific levels to evaluate the spatial turnover at the local scale (i.e.
158 <10 km, following scale definitions of Pearson & Dawson, 2003) and in two habitat
159 types within the same spatial settings. Using the three regions as natural replicates, we
160 evaluated patterns of richness, endemism, turnover and the spatial scale of the distance
161 decay in community similarity at each hierarchical level and assessed the prevailing
162 ecological and evolutionary processes that determine the diversity and spatial
163 distribution of soil arthropod communities at the local scale.

164

165 **MATERIALS AND METHODS**

166 **Soil sampling and mesofauna extraction**

167 A total of 144 soil samples were collected from three regions in the southern Iberian
168 Peninsula at Sierra de Grazalema, (GRA), Sierra de Alatoz (ALZ) and Sierra de la

169 AlcarriaConquense (CUE) (Fig. 1 A). In each region, 24 points were sampled, half of
170 them in *Quercus* forest and half in wet grassland habitat, at distances of 500 m to a
171 maximum of 15 km (Fig. 1, Table S1). For each point, we collected i) a sample
172 containing the superficial soil layer (SUP), by extracting one square meter of leaf litter
173 and humus up to 5 cm deep and ii) a sample of the corresponding deep soil layer
174 (DEEP), by digging the substrate of a 30 cm diameter core to 30 cm depth, comprising
175 ca. 20 litres of soil. Samples were sifted in the field (1cm wire mesh sieve) to remove the
176 biggest vegetation fragments and stones, and subsequently processed following the
177 flotation–Berlese–flotation protocol (FBF) of Arribas et al. (2016) (see below for
178 further details). Within each region and habitat, sampling points were located in natural
179 patches of similar dominant vegetation and elevation. Different variables characterising
180 the sampling points were recorded including elevation, slope, orientation, stoniness,
181 humus depth, qualitative porosity, roots, soil temperature and soil relative humidity
182 (Table S1).

183 After sifting, samples were processed following the flotation–Berlese–flotation
184 protocol (FBF, Arribas et al. 2016) for the ‘clean’ extraction of arthropod mesofauna
185 from a large volume of soil. Briefly, the FBF protocol is based on the flotation of soil in
186 water, which allows the extraction of the organic (floating) matter containing the soil
187 mesofauna from raw soil samples. Subsequently, the organic portion is placed in a
188 modified Berlese apparatus to capture specimens alive and preserve them in absolute
189 ethanol. The last part of the FBF protocol includes additional flotation and filtering
190 steps of the ethanol-preserved arthropods using 1-mm and 0.45- μ m wire mesh sieves to
191 remove debris and dirt accumulated in the Berlese extract. This procedure generates two
192 ‘clean’ subsamples of bulk specimens for DNA extraction, one including all adult and

193 larval Coleoptera, and a second with the smallest mesofauna typically dominated by
194 mites and springtails.

195 **DNA extraction, PCR amplification and Illumina sequencing**

196 Each bulk specimen subsample was independently homogenised and a DNA extraction
197 was performed using the DNeasy Blood and Tissue Spin-Column Kit (Qiagen). DNA
198 extracts were quantified using Nanodrop 8000 UV-Vis Spectrophotometer (Thermo
199 Scientific) and the corresponding subsample pairs were combined at a ratio of 1:10 in
200 the amount of DNA for Coleoptera to Acari plus Collembola (according to the range of
201 expected species diversity of these two fractions), in order to minimise the biomass bias
202 in the sequencing depth of the two mesofauna components. For metabarcoding, the bc3'
203 fragment corresponding to 418 bp of the 3' end of the COI barcode region was
204 amplified. Primers included a tail corresponding to the Illumina P5 and P7 sequencing
205 adapters for subsequent library preparation (see Arribas et al., 2016). For each sample,
206 three independent PCR reactions were performed and the amplicons were pooled. All
207 information regarding primers and PCR reagents and conditions is given in Table S2.
208 Amplicon pools were cleaned using Ampure XP magnetic beads, and used as template
209 for a limited-cycle secondary PCR amplification to add dual-index barcodes and the
210 Illumina sequencing adapters (Nextera XT Index Kit; Illumina, San Diego, CA, USA).
211 The resulting metabarcoding libraries were sequenced on an Illumina MiSeq sequencer
212 (2 x 300 bp paired-end reads) on ~ 1% of the flow cell each, to produce paired reads
213 (R1 and R2) with a given dual tag combination for each sample. Negative controls were
214 maintained across all the different steps above and were sequenced as three independent
215 metabarcoding libraries.

216 **Bioinformatics read processing**

217 Raw reads were quality checked in Fastqc(Babraham Institute, 2013). Primers were
218 trimmed using fastx_trimmer and reads were processed in Trimmomatic(Bolger, Lohse,
219 & Usadel, 2014) using TRAILING:20. Based on results from (Andújar, Arribas, Gray,
220 et al., 2018) on the test of multiple tools and parameters for diverse metazoan
221 metabarcoding samples, we further processed each library independently following
222 several steps of the Usearch(Edgar, 2013) pipeline: reads were merged (option
223 mergepairs – -fastq_minovlen50, -fastq_maxdiffs 15), quality-filtered (Maxee = 1),
224 trimmed to full length amplicons of 418 bp (-sortbylength), dereplicated (-
225 fastx_uniques) and denoised (-unoise3, -minsize 4). Denoised reads from the 48
226 libraries for each region, representing putative haplotypes, were combined and
227 dereplicated to get a collection of unique sequences for each regional dataset. The
228 surviving reads were assigned to high-level taxonomic categories with the lowest
229 common ancestor (LCA) algorithm implemented in MEGAN V5 (Huson, Auch, Qi, &
230 Schuster, 2007). Each read was subjected to BLAST searches (blastn -outfmt 5 -evalue
231 0.001) against a reference library including the NCBI *nt* database (Accessed December
232 2016) plus 382 sequences corresponding to Acari and Collembola collected at Sierra de
233 Grazalema. BLAST matches were fed into MEGAN to compute the taxonomic affinity
234 of each read. This high level taxonomic assignment allowed extracting reads
235 corresponding to the three target groups Acari, Collembola and Coleoptera, while
236 excluding other taxa present in the bulk samples. Reads corresponding to the target
237 groups were then aligned in Geneious 7.1.9(<https://www.geneious.com/>) using MAFFT
238 and the Translation Align options, and those with insertions, deletions or stop codons
239 disrupting the reading frame were identified and subsequently excluded.

240 Haplotypes from each region were further filtered to remove likely nuclear
241 mitochondrial (numts) pseudogenes, following a protocol based on the relative

242 abundance of co-distributed reads (Andújar et al., 2020). The set of putative haplotypes
243 for Acari, Collembola and Coleoptera was used to generate a community table with
244 read-counts (haplotype abundance) by sample against the complete collection of reads
245 (i.e., reads before the dereplicating and denoising steps) using Usearch (-search_exact
246 option). Using these abundances, we firstly removed from each library those haplotypes
247 with four or fewer reads according to the criteria used for the denoising (see above).
248 Next, we identified haplotypes that, in all the libraries where they were present,
249 contributed less than 1% of the total reads of the library. All reads falling in this
250 category were then removed from the analysis, as an auxiliary criterion to define
251 spurious copies not representing the true mitochondrial haplotypes. The 1% cut-off
252 value removes most of the spurious reads while maximizing the number of real
253 haplotypes to be further analysed (see Andújar et al., 2020 for details). Community
254 tables of fully filtered haplotypes were then transformed into incidence
255 (presence/absence) data, that added to the haplotype filtering before, resulting in
256 normalised samples for further analyses.

257 **Analysis of community composition and assembly at multiple thresholds of genetic** 258 **similarity**

259 The analyses were performed using the R-packages vegan (Oksanen et al., 2013),
260 cluster, PMCMR, hier.part, ecodist, and betapart (Baselga & Orme, 2012). The set of
261 filtered haplotypes was used to generate a UPGMA tree with corrected genetic distances
262 (F84 model), and based on this tree all haplotypes were grouped into clusters of genetic
263 similarity at different thresholds (1%, 2%, 3%, 4%, 5%, 6% and 8%). This grouping
264 procedure based on patristic pairwise distances over a phylogenetic tree including all
265 haplotype sequences provided multiple hierarchical levels that each can be used to
266 estimate alpha diversity (Figure 1 provides a graphical abstract of the workflow). These

267 diversity measures were estimated for the richness of lineages by sample for the whole
268 mesofauna community and also for the subsets corresponding to Acari, Collembola and
269 Coleoptera. To test for significant differences in alpha diversity between the
270 communities of different habitats and soil layers of each sampling point, repeated-
271 measures ANOVAs were conducted using habitat and soil layer as grouping factors and
272 sampling point as a within-subjects factor. For each of the three local settings, total
273 accumulative richness (local scale richness) by habitat and soil layer and the
274 contribution of mites, springtails and beetles was also calculated for the various levels
275 of genetic similarity. Endemicity by sampling point was computed for each hierarchical
276 level (once DEEP and SUP samples were combined) as the lineages present exclusively
277 at a single sampling point in the region divided by the total number of lineages found in
278 the region. To assess whether the endemicity by sampling point differed between the
279 communities of forests and grasslands, Wilcoxon tests were conducted using habitat as
280 a grouping factor. For each of the three local settings, the local scale endemicity,
281 defined as the lineages present exclusively at a particular sampling point divided by the
282 total number of lineages in that community, was also calculated for the multiple levels
283 of genetic similarity.

284 For the multi-hierarchical assessment of the variation in community composition
285 at the local scale, the community dissimilarity matrices were generated for total beta
286 diversity (Sorensen index, β_{sor}) and its additive turnover (Simpson index, β_{sim}) and
287 nestedness (β_{sne}) components (Baselga, 2010), for each level of genetic similarity.
288 Community composition matrices were also used for non-parametric multidimensional
289 scaling (NMDS) and plots were created with the *ordispider* option to visualise the
290 compositional ordination of the communities according to the respective habitat and soil
291 layer. To assess for significant differences, permutational ANOVAs were conducted

292 over the community dissimilarity matrices using 999 permutations and the habitat and
293 the soil layer as grouping factors and sampling point as a within-subjects factor. The
294 significant relationships between the dissimilarity matrices generated for the Acari,
295 Collembola and Coleoptera were assessed independently by permutational multiple
296 regression on distance matrices (MRM). Additional NMDS ordinations and
297 permutational ANOVAs were also conducted for each taxonomic group using the same
298 parameters as given before.

299 The analysis of the variation in community composition with spatial distance
300 followed the ‘multi-hierarchical macroecology’ approach of (Baselga et al., 2013)
301 which is based on the joint analysis of distance decay of similarity patterns across the
302 different genetic levels. For each local setting and habitat, the relationship of
303 community similarity between pairs of points (1 – pairwise beta diversity, see above)
304 with their spatial distance (computed in kilometres as the Euclidean distance) was
305 assessed independently at each level of genetic similarity (from haplotypes to 8%
306 lineages). A negative exponential function was used to adjust a generalized linear model
307 (GLM) with Simpson similarity as response variable, spatial distance as predictor, log
308 link and Gaussian error, and maintaining the spatial distances untransformed (Gómez-
309 Rodríguez & Baselga, 2018). Finally, the existence of a fractal pattern (power law
310 function) in the distance-decay curves across the levels of genetic similarity was
311 assessed by a log–log Pearson correlation of genetic level and, independently: (a)
312 number of lineages, (b) initial similarity, and (c) mean similarity. High correlation
313 values are indicative of self-similarity in lineage branching (i.e., number of lineages)
314 and/or spatial geometry of lineage distributional ranges (i.e., initial and mean similarity;
315 Baselga et al., 2015), which are predicted under a neutral process of community
316 evolution.

317 In an equivalent way, these analyses were also conducted to assess the
318 relationships of community similarity and environmental distance as computed using
319 Gower's distance over the recorded variables characterising the sampling points (Table
320 S1). In the cases where this relationship was significant, variance partitioning was
321 conducted to assess the fractions of variance in community dissimilarity that are
322 uniquely and jointly explained by spatial and environmental distance.

323

324 **RESULTS**

325 **Multi-hierarchical assessment of alpha and gamma diversity of soil mesofauna**

326 Processing of 144 soil samples using the FBF protocol, followed by double dual
327 indexing of *coxI* amplicons and Illumina MiSeq sequencing, produced 51433 to 375211
328 sequence reads per sample for GRA, 11307 to 159244 for ALZ, and 43562 to 128149
329 for CUE. Filtering of raw reads using standard protocols of read curation and denoising,
330 followed by removal of likely nuclear mitochondrial pseudogenes generated a
331 conservative set of clean sequences representing the mitochondrial haplotypes. A total of
332 1124, 1009 and 992 haplotypes were found for the GRA, ALZ and CUE local areas
333 respectively, and these numbers declined rapidly when haplotypes were grouped at
334 increasing threshold values, e.g. 511, 479 and 480 lineages at 3% similarity (Table 1),
335 but they declined only slightly further at the higher thresholds, indicating the point at
336 which stable groups are obtained that broadly could represent the species level. The
337 relative proportions of mites, springtails and beetles were similar across the three local
338 settings and hierarchical levels, with Acari representing the richest group (around the
339 50% of clusters) followed by Collembola and Coleoptera in similar proportions (Table
340 1). The taxonomic composition of the samples as estimated by MEGAN is provided in
341 Fig. S1 and included a total of 39, 44 and 40 families of Acari, 11, 9, and 10 families of

342 Collembola and 18, 23 and 20 families of Coleoptera for the GRA, ALC and CUE local
343 settings respectively.

344 The patterns of richness by sample (alpha diversity) for the different habitats,
345 soil layers and genetic thresholds were similar for the three regions, with mean values
346 between 35 - 60 haplotypes and 25 - 42 lineages at 3% per sample (Fig. 2 A, B, C and
347 Fig. S2). Superficial soils had significantly higher diversity than their corresponding
348 deep soil counterparts for the overall dataset and for both of the forest and grassland
349 habitats assessed independently (Fig. 2 A, B, C, Fig S2 and Table S3). At GRA, forest
350 habitat showed significantly higher alpha diversity per sample than grassland. However,
351 no significant differences between forest and grassland were found for ALZ and CUE
352 (Fig. 2 A, B, C and Fig S2, Table S3).

353 The local-scale cumulative richness at each region (gamma diversity) showed
354 more diverse communities for the superficial compared with deep layers, and gamma
355 diversity was generally higher for forest than grassland habitats, but the differences
356 between both habitat types were lower than observed for alpha diversity. Thus, species
357 accumulation was higher for the grassland than forest habitats, and the grassland
358 superficial layers had the highest total richness of haplotypes for ALZ and CUE, and the
359 highest for the three regions at the 3% similarity level (Fig. 2 D, E, F and Fig S3).
360 Patterns of alpha and gamma diversity for the subsets of mites, springtails and beetles
361 were similar (Fig. S3 and S4).

362 **Multi-hierarchical assessment of beta diversity and endemism of soil mesofauna**

363 Compositional dissimilarity of communities within each of the three regions was high
364 and was dominated by lineage turnover β_{sim} , instead of nestedness β_{sne} ($0.8 > \beta_{sim} > 0.95$),
365 across all hierarchical levels. NMDS showed a consistent pattern of the forest and
366 grassland habitats as the main driver of the ordination while soil layers had a secondary

367 role (Fig. 3, Fig. S5). Accordingly, for the three regions and all genetic levels, the
368 community composition was significantly different for both habitats and soil layers but
369 the proportion of variance explained by the forest-grassland factor was always higher
370 (Fig. 3 and Table S4). Beta diversity matrices for mites, springtails and beetles showed
371 high and significant correlations for each of the genetic similarity levels (Table S5), and
372 when independently analysed, these main taxonomic groups each showed similar
373 patterns of community composition.

374 Community similarity (1-pairwise beta diversity) significantly decreased with
375 spatial distance (distance decay) at all levels of genetic similarity for both the forest and
376 grassland habitats, and these patterns were remarkably consistent across the three local
377 settings (Fig. 4, Table S6). The slopes of the exponential decay curves were very similar
378 at all threshold levels, and assemblage similarity increased with each level (Fig. 4, Table
379 S6). The levels of genetic similarity showed a high and significant log-log correlation
380 with the number of lineages ($0.90 <r^2> 0.96, p < 0.001$), initial similarity ($0.86 <r^2>$
381 $0.96, p < 0.001$) and mean similarity of communities ($0.89 <r^2> 0.95, p < 0.001$) for all
382 three regions and two habitats, as expected if community variation across genetic
383 similarity levels can be described by a fractal geometry (Baselga et al., 2013, 2015).

384 Comparisons of distance-decay relationships between forests and grasslands
385 showed similar values for explained variance and for the slopes for the three regions
386 (Fig. 4, Table S6). However, there was a consistent pattern of a lower initial community
387 similarity in grasslands than in forests, particularly above the haplotype level (Fig. 4).
388 Similarly, the local-scale (mean) dissimilarity of communities was always higher for
389 grasslands than for forests and the differences between both increased across the levels
390 of genetic similarity (Fig. 5 A, B, C). A decrease in community similarity with
391 environmental distance was only significant in the case of the forests from ALZ and

392 CUE. However, even in these two significant cases, the variance partitioning showed
393 that uniquely explained variance in environmental distance, i.e. independently of the
394 spatial distance, was low (5 – 9 % of explained variation at all levels) compared with
395 the uniquely explained variance in spatial distance (23 – 31 % of explained variation).

396 The endemicity within the GRA, ALZ and CUE regions ranged from 71%, 64%
397 and 58% at the haplotype level to 55%, 53% and 46% for lineages at the 3% threshold,
398 respectively (Table 1). Comparisons between forest and grassland habitats showed that
399 the local scale endemicity of grassland communities was higher in the case of GRA and
400 CUE and was similar in both habitats for ALZ (Fig. 5 D, E, F). The endemicity by
401 sampling points was consistently higher for grassland than for forest local communities
402 particularly above the haplotype level, although the differences were significant only in
403 the case of the GRA localities (Fig. 5 G, H, I).

404

405 **DISCUSSION**

406 In total, soil samples from three Iberian mountain regions produced over 1000 putative
407 species (lineages at 3%) and nearly 3000 haplotypes of mites, springtails and
408 beetles. Their distribution was determined across numerous sampling points,
409 demonstrating the power of mitochondrial cMBC to overcome impediments to studying
410 the arthropod mesofauna of the soil using conventional morphological and molecular
411 approaches. Data analysis revealed a strong spatial community structure and high levels
412 of endemicity at haplotype, species and supra-specific levels, even at sampling points
413 that were mostly within a few kilometres of each other (maximum 15 km). Patterns of
414 turnover and endemicity were similar in all three independent study regions and in the
415 grassland and forest biomes (that each harbour largely non-overlapping communities).
416 Distance decay is evident at all hierarchical levels, and can be described as self-similar.

417 The correlation of community turnover at population and species levels is expected if
418 soil arthropod assemblages are predominantly driven by distance-based parameters,
419 and movement is strongly constrained at the local scale and over time. In addition, the
420 overriding importance of habitat-related processes was apparent from the strong
421 differentiation of grassland and forest communities, which again was seen recurrently in
422 each of the three study regions.

423 The study extends existing comparative analyses of soil mesofauna by improving
424 the taxonomic resolution, providing haplotype level variation, and analysing a wide
425 range of soil arthropods together. Broad surveys of invertebrate soil diversity using HTS
426 have commonly relied on markers of low species-level resolution and via eDNA
427 extracted from small soil samples (Bahram et al., 2016; Wu et al., 2011; Zinger et al.,
428 2019). Other studies have characterised specific groups of mites or springtails by
429 processing of individualised specimens and relying on morphological assignment to
430 generate species-level data (Caruso, Schaefer, Monson, & Keith, 2019; Ingimarsdóttir et
431 al., 2012), but see also Young, Proctor, DeWaard, & Hebert (2019) on molecular species
432 assignment. HTS data now greatly increase the potential of expanding both the number
433 of species studied and the level of detail at which intra-specific variation for each is
434 captured. Our study provides haplotype level data for entire communities (one square
435 meter of leaf litter and humus and ca. 20 litres of soil per sampling point) of the three
436 most species-rich soil arthropods, which allows surveys of community composition and
437 species turnover at an unprecedented level of detail, both spatially and genetically.
438 While the correlation of COI divergence with species boundaries can vary greatly
439 between taxa, we analysed our dataset using an extensive range of hierarchical
440 thresholds (from 1 to 8% genetic similarity thresholds) as a simplified but conservative
441 approach to consider both species and supra-specific levels. We found some degree of

442 stabilization in the number of lineages defined above the 3% similarity grouping,
443 consistent with this similarity threshold as broadly representing the species level. Using
444 these data, community level responses to distance-based parameters can be assessed that
445 may be not evident in other types of studies. In addition, the combined haplotype and
446 species-level data permit the exploitation of the hierarchical framework of Baselga et al.
447 (2013, 2015) for discriminating between distance- and niche-based factors of
448 community assembly.

449 *The limited spatial scale of dispersal in soil arthropods*

450 Existing literature exploring the local community composition of arthropod
451 mesofauna generally has argued for selection by abiotic and/or biotic environmental
452 factors as the predominant mechanisms (see Berg, 2012; Thakur et al., 2019 for a recent
453 review). Stochastic and purely spatial patterns have also been reported, pointing to a
454 contribution of dispersal and demographic processes at least in some local
455 settings (Caruso et al., 2012; Gao et al., 2014; Gao, Liu, Lin, & Wu, 2016; Zinger et al.,
456 2019). However, strong dispersal constraints have rarely been recognised, in part due to
457 the lower taxonomic resolution of previous community-level studies that used species
458 assignments from morphological or 18S rRNA data (see Tang et al., 2012). Our results
459 demonstrate high community differentiation at the kilometre scale for both genetic and
460 species levels. The key observation from the multi-hierarchical analysis is the correlated
461 distance decay at haplotype and species level. Self-similarity is expected to be eroded
462 by selection on adaptive traits at the species level, but not at the (neutral) haplotype level
463 (Baselga et al., 2015; Gómez Rodríguez et al., 2018). As the data largely confirm the
464 self-similarity of distance decay at haplotype and species level, this is interpreted to
465 support the predominant role of dispersal limitation driving community assembly. The
466 predominance of the dispersal constraints seems to emerge at short spatial distances

467 within the soil matrix, and the evident high turnover with physical distancesuggests that
468 our sampling within each study regions (local scale) is beyond the scale of a single
469 metacommunity. Short dispersal distancesprobably have affected a significant
470 proportion of lineages within these communities over evolutionary timescalesin a
471 largely stable spatial setting.The spatiotemporal continuum expected under this scenario
472 predicts that lineages in more distant places have diverged at a more distanttime point in
473 evolutionary history (Baselga et al., 2013, 2015), and our findings of a largely regular
474 distance decay at higher levels are consistent with this prediction. Additional evidence
475 for the role of short dispersal distancedriving the local community assembly comes
476 from the high microendemicityfound at all hierarchical levels, an overall picture which
477 is not expected under a scenario with predominant environmental driversnor ecological
478 drift without dispersal limitation.

479 Yet, the influence of environmental drivers cannot be discarded entirely.
480 Whereas the recorded environmental variables did not explain the variation in
481 community composition, a significant portion of the unexplained variance in the
482 distance-decay curves potentiallysuggests the influence of non-spatial factors
483 determining the community composition. Edaphic parameters such as soil pH or organic
484 matter have been shown to explain a significant part of the variance observed in the
485 distribution of the soil mesofauna communities(Caruso et al., 2012; Gao et al., 2014),
486 and here could be driving at least part of the unexplained variation within the different
487 habitats and regions. Edaphic environmental variables are often spatially structured and
488 so have been also reported as potential drivers of purely spatial patterns in mesofauna
489 communities (Caruso et al., 2019, 2012). However, this possibility is poorly supported
490 here, as similar spatial structures were independently found within the different habitats
491 and regions, mirroring thedistance-decay patterns at the (neutral) haplotype level, and

492 hence suggesting that dispersal limitation is the main driver of the local spatial structure
493 of the studied mesofauna communities.

494 The small spatial scale of turnover and endemism is consistent with population
495 genetic studies in soil mesofauna showing deep genetic breaks even over relatively
496 short geographic distances (Andújar, Pérez-González, et al., 2017; Cicconardi et al.,
497 2013; Collins, Hogg, Convey, Barnes, & McDonald, 2019). In contrast, our results are
498 not concordant with long-distance dispersal as a prevalent process for soil mesofauna, as
499 might be expected from passive dispersal by air, water or in marine plankton (Decaëns,
500 2010; Thakur et al., 2019; Wardle, 2002). Existing reports of long-distance dispersal are
501 mainly into virgin isolated habitats (Ingimarsdóttir et al., 2012) or
502 recently deglaciated areas (Gan et al., 2019), or may involve the detection of mesofauna
503 during transport (Coulson, Hodkinson, & Webb, 2003; Schuppenhauer et al., 2019).
504 However, they do not inform about colonisation and establishment success (effective
505 dispersal) and possibly only pertain to a few highly dispersive species. Additionally, the
506 dispersal potential may have been overestimated due to the low resolution of
507 morphological species identification (Cicconardi et al., 2013) leading to perceived low
508 turnover among sites, as evident from recent large-scale barcoding studies (Collins,
509 Hogg, Baxter, Maggs-Kölling, & Cowan, 2019; Young et al., 2019). Our results at the
510 community level thus raise doubts about a generalised dispersal advantage for small-
511 bodied arthropods and instead indicate very small dispersal distances, even over
512 evolutionary time scales, for the majority of species that make up the complex
513 mesofauna communities of the soil. This scale and dynamics of community assembly
514 contrasts with patterns and processes reported for the microbial eukaryote diversity of
515 the soil (Bahram et al., 2016) and aligns with recent empirical evidences suggesting that
516 at the local scale dispersal rates may be much lower for soil mesofauna than for

517 microfauna(Zinger et al., 2019).In the context of theoverall arthropod diversity(for
518 which soil mesofauna comprises the majority of the smallest fraction), our results are
519 not supporting the macroecologicalpredictionfora reduce impact of dispersal limitation
520 in the assemblage for small-bodied components compared with their bigger
521 counterparts(de Bie et al., 2012; Ricklefs, 2004)and highlight the uniqueness
522 ofecological and evolutionary processes driving the biodiversity ofthese edaphic
523 arthropods(Andújar, Arribas, & Vogler, 2017; Andújar, Pérez-González, et al., 2017).

524 *The role of dispersal constraints within a habitat-based framework*

525 In spite of the important role of dispersal limitation within each habitat type, the greatest
526 assemblage differentiation was between grassland and forest communities, which share
527 very few species even in close (meters) spatial proximity. Previous studies also have
528 shown great differences in soil arthropod community composition between beech forest
529 and adjacent grassland (Caruso et al., 2012), and twice higher species richness in the
530 forest community. The grassland-forest dichotomy in community composition is
531 concordant with these findings, but the total diversity in either type of community was
532 more complex.Alpha diversity tended to be higher for forest habitats, although lineage
533 accumulation across multiple sites was higher for the grasslands, resulting in higher
534 overall landscape richness (gamma diversity). Grassland communities also had
535 consistently lower initial and mean community similarities in the corresponding
536 distance decay curves, together with higher levels of both point and local scale
537 endemism. These results are recurrent across the three sampling areas and point to
538 slightly higher long-term dispersal constraints for the mesofauna in the grasslands
539 studied.

540 Grassland species are expected to experience higher environmental variability and
541 greater extremes, which are moderated within forested patches and thus presumably are

542 more stable (De Frenne et al., 2019). Under the habitat stability hypothesis (Ribera &
543 Vogler, 2000; Southwood, 1977), low species turnover is predicted in less stable
544 habitats due to the stronger selection on traits promoting dispersal that are required to
545 persist in ephemeral environments. However, our findings are not aligned with this
546 hypothesis, suggesting similar local-scale patterns of lineage turnover within both
547 habitats and with slightly stronger community structure for the presumably less stable
548 grasslands. Further studies comparing the assemblages of both habitat types across
549 gradients of stability (e.g. latitude) are needed to identify the processes driving the
550 mesofaunal community turnover, but both habitat types show the signature of long-term
551 stability without which the high spatial structure at multiple hierarchical levels and
552 between grassland and forest habitats could not have arisen.

553 *Extrapolating beyond the local scale*

554 The recurrence of the local patterns in each of the three study regions and across the
555 three major taxonomic groups corroborates the hypothesis of an underlying process of
556 stochastic dispersal of individuals, affected by a universal type of dispersal constraint.
557 This seems to affect a majority of species composing these communities, regardless of
558 their taxonomic affinity, species traits or functional role. The soil matrix provides a
559 common sphere in which these processes are played out, and if these soils are similar,
560 complex communities, on average, appear to respond in a similar way. The two habitat
561 types clearly provide different overall settings, obvious from the very different species
562 present, but they also impact the respective species pool in similar ways. With the local-
563 scale patterns and likely underlying processes reported here, questions arise about the
564 impact for cross-regional and global spatial scales, and how these patterns and processes
565 compare to aboveground arthropod components. If generalized across broader
566 geographical scales and other ecoregions, the very reduced spatial scale of dispersal in

567 soil mesofauna could be a major contribution to the overall gamma diversity and may
568 lead to a revised estimate of total species diversity on Earth. In this sense, further
569 developments on the multi-hierarchical analysis of genetic and higher-level diversity
570 from metabarcoding data has the potential to propel the characterisation of edaphic
571 microbialcommunity structure into a new era of biodiversity discovery. By taking
572 advantage of the full breadth of contemporary metabarcoding data at expanded
573 taxonomic and geographic scales,the advances made here will provide unique insights
574 into the ecological and evolutionary processes that determine the magnitude and spatial
575 distribution of soil arthropods.

576

577 **ACKNOWLEDGMENTS**

578 This research was funded by Newton International Program, UK to PA and the NHM
579 Biodiversity Initiative to APV. PA was supported by postdoctoral grants from the Royal
580 Society (Newton International Program, UK) and the Spanish Ministry of Economy and
581 Competitiveness (MINECO, Spain) within the Juan de la CiervaFormación Program.
582 CA was supported by the Spanish Ministry of Economy and Competitiveness
583 (MINECO, Spain) (CGL2015-74178-JINMINECO/FEDER, UE). Thanks are due to the
584 regional government of Andalucía and Castilla-la-Mancha (Spain); Alex Aitken, Andie
585 Hall, Stephen Russell and Peter Foster (all NHM) for their technical assistance and to
586 JesúsArribas who assisted with field sampling.

587

588 **REFERENCES**

- 589 Andújar, C., Arribas, P., Gray, C., Bruce, C., Woodward, G., Yu, D. W., & Vogler, A.
 590 P. (2018). Metabarcoding of freshwater invertebrates to detect the effects of a
 591 pesticide spill. *Molecular Ecology*, 27(1), 146–166. doi: 10.1111/mec.14410
- 592 Andújar, C., Arribas, P., Ruzicka, F., Platt, A. C., Timmermans, M. J. T. N. M. J. T. N.
 593 J. T. N., Vogler, A. P. A. A. P., ... Vogler, A. P. A. A. P. (2015). Phylogenetic
 594 community ecology of soil biodiversity using mitochondrial metagenomics.
 595 *Molecular Ecology*, 24(14), 3603–3617. doi: 10.1111/mec.13195
- 596 Andújar, C., Arribas, P., & Vogler, A. P. (2017). Terra incognita of soil biodiversity:
 597 unseen invasions under our feet. *Molecular Ecology*, 26(12), 3087–3089. doi:
 598 10.1111/mec.14112
- 599 Andújar, C., Arribas, P., Yu, D. W., Vogler, A. P., & Emerson, B. C. (2018). Why the
 600 COI barcode should be the community DNA metabarcode for the Metazoa.
 601 *Molecular Ecology*, 27(July), 3968–3975. doi: 10.1111/mec.14844
- 602 Andújar, C., Creed, T. J., Arribas, P., López, H., Salces-Castellano, A., Pérez-Delgado,
 603 A. J., ... Emerson, B. C. (2020). NUMT dumping : validated removal of nuclear
 604 pseudogenes from mitochondrial metabarcode data. *BioRxiv*.
- 605 Andújar, C., Pérez-González, S., Arribas, P., Zaballos, J. P., Vogler, A. P., & Ribera, I.
 606 (2017). Speciation below ground: Tempo and mode of diversification in a radiation
 607 of endogean ground beetles. *Molecular Ecology*, 26(21), 6053–6070. doi:
 608 10.1111/mec.14358
- 609 Arribas, P., Andújar, C., Hopkins, K., Shepherd, M., Vogler, A. P., Andújar, C., ...
 610 Vogler, A. P. A. P. (2016). Metabarcoding and mitochondrial metagenomics of
 611 endogean arthropods to unveil the mesofauna of the soil. *Methods in Ecology and*
 612 *Evolution*, 7(9), 1071–1081. doi: 10.1111/2041-210X.12557
- 613 Babraham Institute. (2013). *FastQC: A quality control tool for high throughput*
 614 *sequence data*. <http://www.bioinformatics.babraham.ac.uk/projects/fastqc>.
- 615 Bahram, M., Kohout, P., Anslan, S., Harend, H., & Abarenkov, K. (2016). Stochastic
 616 distribution of small soil eukaryotes resulting from high dispersal and drift in a
 617 local environment. *ISME Journal*, 10(4), 885–896. doi: 10.1038/ismej.2015.164
- 618 Baird, H. P., Leihy, R. I., Scheepers, C. J., & Chown, S. L. (2019). The ecological
 619 biogeography of indigenous and introduced Antarctic springtails. *Journal of*
 620 *Biogeography*, (April), 1–15. doi: 10.1111/jbi.13639
- 621 Bardgett, R. D., Usher, M. B., & Hopkins, D. W. (2005). *Biological diversity and*
 622 *function in soils*. Cambridge: Cambridge University Press.
- 623 Bardgett, R. D., & van der Putten, W. H. (2014). Belowground biodiversity and
 624 ecosystem functioning. *Nature*, 515(7528), 505–511. doi: 10.1038/nature13855
- 625 Baselga, A. (2010). Partitioning the turnover and nestedness components of beta

- 626 diversity. *Global Ecology and Biogeography*, 19(1), 134–143. doi: 10.1111/j.1466-
627 8238.2009.00490.x
- 628 Baselga, A., Fujisawa, T., Crampton-Platt, A., Bergsten, J., Foster, P. G., Monaghan, M.
629 T., & Vogler, A. P. (2013). Whole-community DNA barcoding reveals a spatio-
630 temporal continuum of biodiversity at species and genetic levels. *Nature*
631 *Communications*, 4(May), 1892. doi: 10.1038/ncomms2881
- 632 Baselga, A., Gómez-Rodríguez, C., & Vogler, A. P. (2015). Multi-hierarchical
633 macroecology at species and genetic levels to discern neutral and non-neutral
634 processes. *Global Ecology and Biogeography*, 873–882. doi: 10.1111/geb.12322
- 635 Baselga, A., & Orme, C. D. L. (2012). betapart: an R package for the study of beta
636 diversity. *Methods in Ecology and Evolution*, 3(5), 808–812. doi: 10.1111/j.2041-
637 210X.2012.00224.x
- 638 Berg, M. P. (2012). Patterns of biodiversity at fine and small spatial scales. In D. H.
639 Wall, R. D. Bardgett, V. M. Behan-Pelletier, & E. Al. (Eds.), *Soil Ecology and*
640 *Ecosystem Services* (pp. 136–152). Oxford: Oxford University Press.
- 641 Bolger, A. M., Lohse, M., & Usadel, B. (2014). Trimmomatic: A flexible trimmer for
642 Illumina sequence data. *Bioinformatics*, 30(15), 2114–2120. doi:
643 10.1093/bioinformatics/btu170
- 644 Cameron, E. K., Martins, I. S., Lavelle, P., Mathieu, J., Tedersoo, L., Gottschall, F., ...
645 Eisenhauer, N. (2018). Global gaps in soil biodiversity data. *Nature Ecology and*
646 *Evolution*, 2(7), 1042–1043. doi: 10.1038/s41559-018-0573-8
- 647 Caruso, T., Schaefer, I., Monson, F., & Keith, A. M. (2019). Oribatid mites show how
648 climate and latitudinal gradients in organic matter can drive large-scale
649 biodiversity patterns of soil communities. *Journal of Biogeography*, 46(3), 611–
650 620. doi: 10.1111/jbi.13501
- 651 Caruso, T., Taormina, M., & Migliorini, M. (2012). Relative role of deterministic and
652 stochastic determinants of soil animal community: a spatially explicit analysis of
653 oribatid mites. *The Journal of Animal Ecology*, 81(1), 214–221. doi:
654 10.1111/j.1365-2656.2011.01886.x
- 655 Caruso, T., Trokhymets, V., Bargagli, R., & Convey, P. (2013). Biotic interactions as a
656 structuring force in soil communities: Evidence from the micro-arthropods of an
657 Antarctic moss model system. *Oecologia*, 172(2), 495–503. doi: 10.1007/s00442-
658 012-2503-9
- 659 Cicconardi, F., Fanciulli, P. P. P., & Emerson, B. C. B. (2013). Collembola, the
660 biological species concept and the underestimation of global species richness.
661 *Molecular Ecology*, 22(21), 5382–5396. doi: 10.1111/mec.12472
- 662 Collins, G. E., Hogg, I. D., Baxter, J. R., Maggs-Kölling, G., & Cowan, D. A. (2019).
663 Ancient landscapes of the Namib Desert harbor high levels of genetic variability
664 and deeply divergent lineages for Collembola. *Ecology and Evolution*, 9(8), 4969–
665 4979. doi: 10.1002/ece3.5103

- 666 Collins, G. E., Hogg, I. D., Convey, P., Barnes, A. D., & McDonald, I. R. (2019).
667 Spatial and temporal scales matter when assessing the species and genetic diversity
668 of springtails (Collembola) in Antarctica. *Frontiers in Ecology and Evolution*,
669 7(MAR), 1–18. doi: 10.3389/fevo.2019.00076
- 670 Coulson, S. J., Hodkinson, I. D., & Webb, N. R. (2003). Microscale distribution patterns
671 in high Arctic soil microarthropod communities: The influence of plant species
672 within the vegetation mosaic. *Ecography*, 26(6), 801–809. doi: 10.1111/j.0906-
673 7590.2003.03646.x
- 674 Coulson, S. J., Hodkinson, I. D., Webb, N. R., & Harrison, J. A. (2002). *Survival of*
675 *terrestrial soil-dwelling arthropods on and in seawater : implications for trans-*
676 *oceanic dispersal*. 353–356.
- 677 de Bie, T., de Meester, L., Brendonck, L., Martens, K., Goddeeris, B., Ercken, D., ...
678 Declerk, S. A. . (2012). Body size and dispersal mode as key traits determining
679 metacommunity structure of aquatic organisms. *Ecology Letters*, 4, 740–747. doi:
680 10.1111/j.1461-0248.2012.01794.x
- 681 De Frenne, P., Zellweger, F., Rodríguez-Sánchez, F., Scheffers, B. R., Hylander, K.,
682 Luoto, M., ... Lenoir, J. (2019). Global buffering of temperatures under forest
683 canopies. *Nature Ecology and Evolution*, 3(5), 744–749. doi: 10.1038/s41559-019-
684 0842-1
- 685 Decaëns, T. (2010). Macroecological patterns in soil communities. *Global Ecology and*
686 *Biogeography*, 19(3), 287–302. doi: 10.1111/j.1466-8238.2009.00517.x
- 687 Delgado-Baquerizo, M., Oliverio, A. M., Brewer, T. E., Benavent-gonzález, A.,
688 Eldridge, D. J., Bardgett, R. D., ... Fierer, N. (2018). Bacteria Found in Soil.
689 *Science*, 325(February), 320–325. doi: 10.1126/science.aap9516
- 690 Edgar, R. C. (2013). UPARSE: highly accurate OTU sequences from microbial
691 amplicon reads. *Nature Methods*, 10(10), 996–998. doi: 10.1038/nmeth.2604
- 692 Elbrecht, V., Vamos, E. E., Steinke, D., & Leese, F. (2018). Estimating intraspecific
693 genetic diversity from community DNA metabarcoding data. *PeerJ*, 6, e4644. doi:
694 10.7717/peerj.4644
- 695 Gan, H., Zak, D. R., & Hunter, M. D. (2019). Scale dependency of dispersal limitation,
696 environmental filtering and biotic interactions determine the diversity and
697 composition of oribatid mite communities. *Pedobiologia*, 74(June 2017), 43–53.
698 doi: 10.1016/j.pedobi.2019.03.002
- 699 Gao, M., He, P., Zhang, X., Liu, D., & Wu, D. (2014). Relative roles of spatial factors,
700 environmental filtering and biotic interactions in fine-scale structuring of a soil
701 mite community. *Soil Biology and Biochemistry*, 79, 68–77. doi:
702 10.1016/j.soilbio.2014.09.003
- 703 Gao, M., Liu, D., Lin, L., & Wu, D. (2016). The small-scale structure of a soil mite
704 metacommunity. *European Journal of Soil Biology*, 74, 69–75. doi:
705 10.1016/j.ejsobi.2016.03.004

- 706 Gómez-Rodríguez, C., & Baselga, A. (2018). Variation among European beetle taxa in
707 patterns of distance decay of similarity suggests a major role of dispersal
708 processes. *Ecography*, *41*(11), 1825–1834. doi: 10.1111/ecog.03693
- 709 Gómez-Rodríguez, C., Miller, K. E., Castillejo, J., Iglesias-Peireiro, J., & Baselga, A.
710 (2018). Understanding dispersal limitation through the assessment of diversity
711 patterns across phylogenetic scales below the species level. *Global Ecology and*
712 *Biogeography*, (October), 1–12. doi: 10.1111/geb.12857
- 713 Hortal, J., Roura-Pascual, N., Sanders, N. J., & Rahbek, C. (2010). Understanding
714 (insect) species distributions across spatial scales. *Ecography*, *33*(1), 51–53. doi:
715 10.1111/j.1600-0587.2009.06428.x
- 716 Huson, D. H., Auch, A. F., Qi, J., & Schuster, S. C. (2007). MEGAN analysis of
717 metagenomic data. *Genome Research*, *17*(3), 377–386. doi: 10.1101/gr.5969107
- 718 Ingimarsdóttir, M., Caruso, T., Ripa, J., Magnúsdóttir, O. B., Migliorini, M., &
719 Hedlund, K. (2012). Primary assembly of soil communities: disentangling the
720 effect of dispersal and local environment. *Oecologia*, *170*(3), 745–754. doi:
721 10.1007/s00442-012-2334-8
- 722 Ji, Y., Ashton, L., Pedley, S. M., Edwards, D. P., Tang, Y., Nakamura, A., ... Yu, D. W.
723 (2013). Reliable, verifiable and efficient monitoring of biodiversity via
724 metabarcoding. *Ecology Letters*, *16*(10), 1245–1257. doi: 10.1111/ele.12162
- 725 Lindo, Z., & Winchester, N. N. (2009). Spatial and environmental factors contributing
726 to patterns in arboreal and terrestrial oribatid mite diversity across spatial scales.
727 *Oecologia*, *160*(4), 817–825. doi: 10.1007/s00442-009-1348-3
- 728 Magilton, M., Maraun, M., Emmerson, M., & Caruso, T. (2019). Oribatid mites reveal
729 that competition for resources and trophic structure combine to regulate the
730 assembly of diverse soil animal communities. *Ecology and Evolution*, *9*(14), 8320–
731 8330. doi: 10.1002/ece3.5409
- 732 Múrria, C., Bonada, N., Vellend, M., Zamora-Muñoz, C., Alba-Tercedor, J., Sainz-
733 cantero, C. E. C. E., ... Vogler, A. P. (2017). Local environment rather than past
734 climate determines community composition of mountain stream
735 macroinvertebrates across Europe a. *Molecular Ecology*, *26*(May), 6085–6099.
736 doi: 10.1111/mec.14346
- 737 Nkem, J. N., Wall, D. H., Virginia, R. A., Barrett, J. E., Broos, E. J., Porazinska, D. L.,
738 & Adams, B. J. (2006). Wind dispersal of soil invertebrates in the McMurdo Dry
739 Valleys, Antarctica. *Polar Biology*, *29*(4), 346–352. doi: 10.1007/s00300-005-
740 0061-x
- 741 Oksanen, J., Blanchet, F. G., Kindt, R., Legendre, P., Minchin, P. R., O’Hara, R. B., ...
742 Wagner, H. (2013). Vegan: Community Ecology Package. R package version 2.0-
743 10. <http://cran.r-project.org/package=vegan>. *R Package Ver. 2.0–8*, p. 254.
- 744 Pearson, R. G., & Dawson, T. P. (2003). Predicting the impacts of climate change on
745 the distribution of species: are bioclimate envelope models useful? *Global Ecology*
746 *and Biogeography*, *12*(5), 361–371. doi: 10.1046/j.1466-822X.2003.00042.x

- 747 Ramirez, K. S., Knight, C. G., De Hollander, M., Brearley, F. Q., Constantinides, B.,
748 Cotton, A., ... De Vries, F. T. (2018). Detecting macroecological patterns in
749 bacterial communities across independent studies of global soils. *Nature*
750 *Microbiology*, 3(2), 189–196. doi: 10.1038/s41564-017-0062-x
- 751 Ramirez, K. S., Leff, J. W., Barberán, A., Bates, S. T., Betley, J., Thomas, W., ...
752 Fierer, N. (2014). Biogeographic patterns in below-ground diversity in New York
753 City ' s Central Park are similar to those observed globally Biogeographic patterns
754 in below-ground diversity in New York City ' s Central Park are similar to those
755 observed globally. *Proceedings of the Royal Society B*, 281, 20141988. doi:
756 <http://dx.doi.org/10.1098/rspb.2014.1988>
- 757 Ribera, I., & Vogler, A. P. (2000). Habitat type as a determinant of species range sizes:
758 the example of lotic-lentic differences in aquatic Coleoptera. *Biological Journal of*
759 *the Linnean Society*, 71(1), 33–52. doi: 10.1111/j.1095-8312.2000.tb01240.x
- 760 Ricklefs, R. E. (2004). A comprehensive framework for global patterns in biodiversity.
761 *Ecology Letters*, 7(1), 1–15. doi: 10.1046/j.1461-0248.2003.00554.x
- 762 Schuppenhauer, M. M., Lehmitz, R., & Xylander, W. E. R. (2019). Slow-moving soil
763 organisms on a water highway: Aquatic dispersal and survival potential of
764 Oribatida and Collembola in running water. *Movement Ecology*, 7(1), 1–14. doi:
765 10.1186/s40462-019-0165-5
- 766 Southwood, T. R. E. (1977). Habitat, the templet for ecological strategies? *Journal of*
767 *Animal Ecology*, 46(2), 336–365.
- 768 Tang, C. Q., Leasi, F., Obertegger, U., Kieneke, a., Barraclough, T. G., & Fontaneto,
769 D. (2012). The widely used small subunit 18S rDNA molecule greatly
770 underestimates true diversity in biodiversity surveys of the meiofauna.
771 *Proceedings of the National Academy of Sciences*, 109(40), 16208–16212. doi:
772 10.1073/pnas.1209160109
- 773 Thakur, M. P., Phillips, H. R. P., Brose, U., De Vries, F. T., Lavelle, P., Loreau, M., ...
774 Cameron, E. K. (2019). Towards an integrative understanding of soil biodiversity.
775 *Biological Reviews*, 31, brv.12567. doi: 10.1111/brv.12567
- 776 Turon, X., Antich, A., Palacín, C., Præbel, K., & Wangenstein, O. S. (2019). From
777 metabarcoding to metaphylogeography: separating the wheat from the chaff.
778 *BioRxiv*, (May), 629535. doi: 10.1101/629535
- 779 Wardle, D. A. (2002). *Communities and Ecosystems: Linking the aboveground and*
780 *belowground components*. Princeton: Princeton University Press.
- 781 Widenfalk, L. A., Malmström, A., Berg, M. P., & Bengtsson, J. (2016). Small-scale
782 Collembola community composition in a pine forest soil – Overdispersion in
783 functional traits indicates the importance of species interactions. *Soil Biology and*
784 *Biochemistry*, 103, 52–62. doi: 10.1016/j.soilbio.2016.08.006
- 785 Wu, T., Ayres, E., Bardgett, R. D., Wall, D. H., & Garey, J. R. (2011). Molecular study
786 of worldwide distribution and diversity of soil animals. *Proceedings of the*
787 *National Academy of Sciences of the United States of America*, 108(43), 17720–

- 788 17725. doi: 10.1073/pnas.1103824108
- 789 Young, M. R., Proctor, H. C., DeWaard, J. R., & Hebert, P. D. N. (2019). DNA
790 Barcodes Expose Unexpected Diversity in Canadian Mites. *Molecular Ecology*, 0–
791 2. doi: 10.1111/mec.15292
- 792 Zinger, L., Taberlet, P., Schimann, H., Bonin, A., Boyer, F., De Barba, M., ... Chave, J.
793 (2019). Body size determines soil community assembly in a tropical forest.
794 *Molecular Ecology*, 28(3), 528–543. doi: 10.1111/mec.14919
- 795

796 **DATA ACCESSIBILITY STATEMENT**

797 Raw metabarcoding data deposited in the Dryad repository:

798 <https://doi.org/10.5061/dryad.vx0k6djph>; primers and PCR conditions in Table S2; all

799 supplementary tables and figures cited in the main text have been uploaded as online

800 Supporting Information.

801

802 **AUTHOR CONTRIBUTIONS**

803 Statement of authorship: P.A., C.A. and A.P.V. conceived the work; P.A. and C.A.

804 collected and analysed the data; P.A led the writing and all authors contributed to the

805 discussion of results and the writing.

806

807 **Table 1** Total number of haplotypes and clusters for Acari, Collembola and Coleoptera
 808 for each local setting (GRA, ALZ, CUE) at increasing levels of genetic divergence
 809 thresholds.

	haplotypes	1% lineages	2% lineages	3% lineages	4% lineages	5% lineages	6% lineages	8% lineages
GRA								
Total	1124	693	559	511	487	470	458	436
<i>Acari</i>	540	354	286	260	243	233	226	219
<i>Collembola</i>	306	172	129	113	108	104	101	94
<i>Coleoptera</i>	278	167	144	138	136	133	131	123
ALZ								
Total	1009	655	540	479	451	431	419	407
<i>Acari</i>	451	319	260	226	210	197	194	189
<i>Collembola</i>	275	155	114	94	90	87	81	77
<i>Coleoptera</i>	283	181	166	159	151	147	144	141
CUE								
Total	992	613	519	480	462	443	437	423
<i>Acari</i>	459	296	244	220	208	198	193	184
<i>Collembola</i>	273	138	117	107	101	96	95	91
<i>Coleoptera</i>	260	179	158	153	153	149	149	148

810

811

812 **FIGURE CAPTIONS**

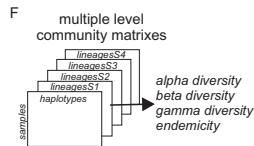
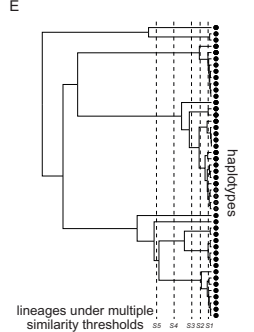
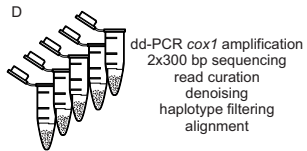
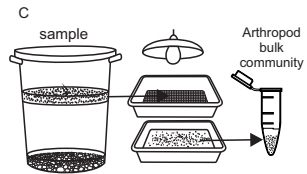
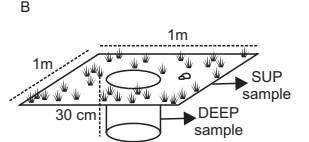
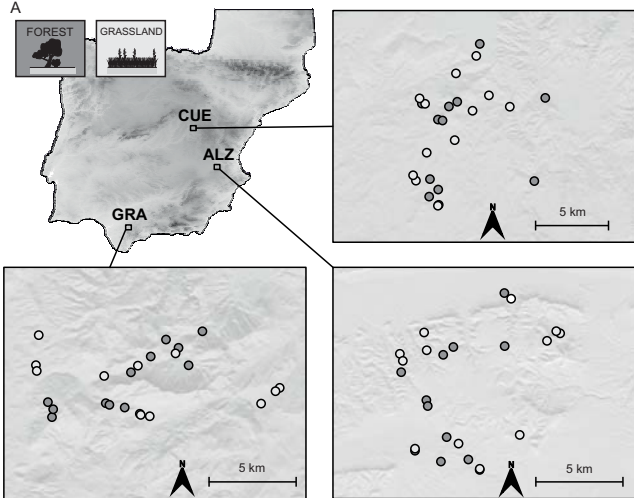
813 **Figure 1.** Sampling points in the three local settings within the Iberian Peninsula, Sierra
814 de Grazalema, (GRA), Sierra de Alatoz (ALZ) and Sierra de la AlcarriaConquense
815 (CUE). Sampling points are located within *Quercus* forest patches (dark grey) and wet
816 grassland patches (pale grey).

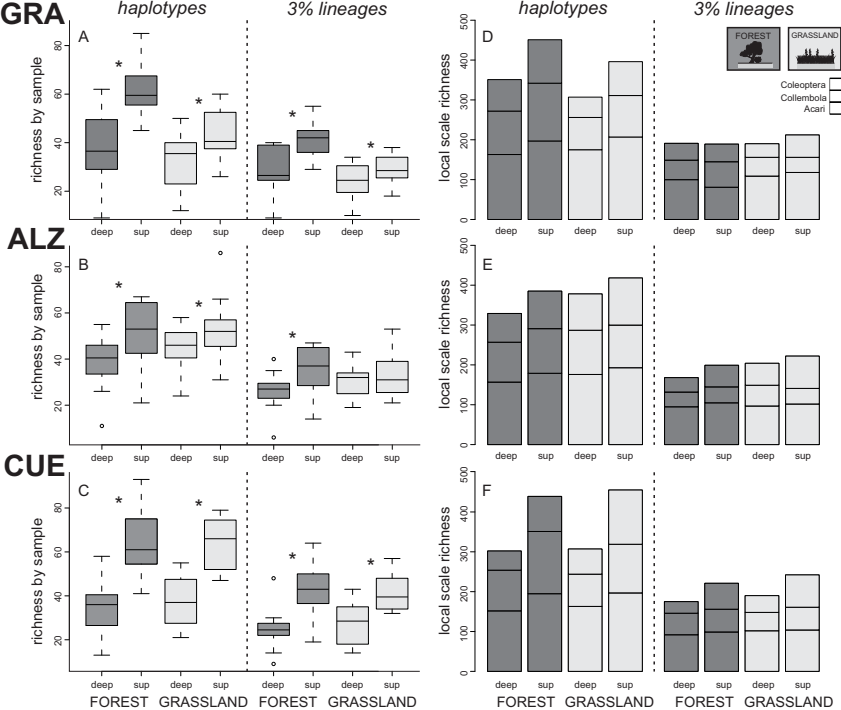
817 **Figure 2.** Richness of soil mesofauna lineages by sample (alpha diversity, A, B, C) and
818 total accumulated richness (local scale richness, D, E, F) by habitat and soil layer for the
819 three local settings (GRA, ALZ, CUE). Both measures are shown at the haplotype and
820 the 3% genetic similarity levels. Forest habitat as dark grey, grassland habitat as pale
821 gray, sup for superficial and deep for deep soil layers. Significantly different richness of
822 lineages by sample (repeated-measures ANOVA $p < 0.05$) between deep and superficial
823 communities of each habitat are indicated by asterisks within A, B, C panels. The
824 contribution of Acari, Collembola and Coleoptera to the local scale richness are shown
825 within D, E, F panels.

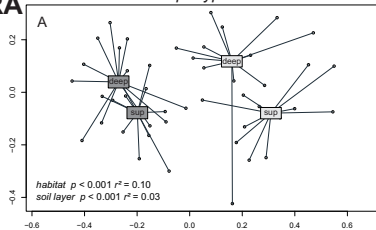
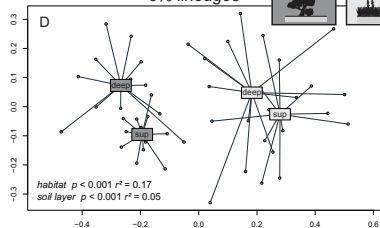
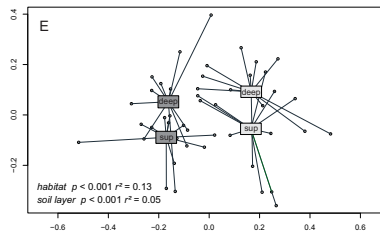
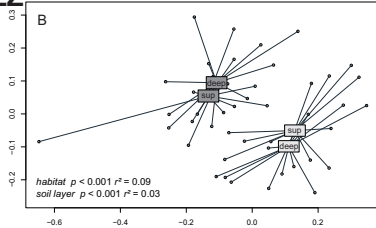
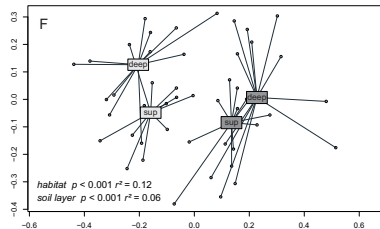
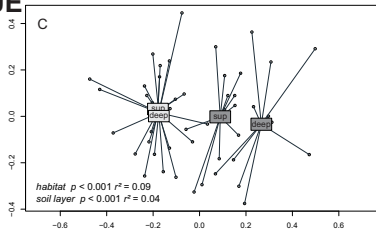
826 **Figure 3.** NMDS ordinations of the soil mesofauna samples according to the variation
827 in community composition (Simpson index, β_{sim}) within the three local settings (GRA,
828 ALZ, CUE) and at the haplotype and the 3% genetic similarity levels. Forest habitat as
829 dark grey, grassland habitat as pale grey, sup for superficial and deep for deep soil
830 layers. Explained variation (r^2) and significance (p) of each grouping factor from the
831 permutational ANOVAs over the community dissimilarity matrixes are shown.

832 **Figure 4.** Distance decay of soil mesofauna community similarity at multiple levels of
833 genetic similarity (from haplotype, black to 8% genetic similarity level, pale grey)
834 within the three local settings (GRA, ALZ, CUE) and for forest and grassland habitats.

835 **Figure 5.** Dissimilarity of soil mesofauna communities (A, B, C), regional endemicity
836 (lineages present exclusively at a single sampling point in the region divided by the total
837 number of lineages found, D, E, F) and endemicity by sampling points (lineages present
838 exclusively at a particular sampling point divided by the total number of lineages in that
839 community, G, H, I) at multiple levels of genetic similarity within the three local
840 settings (GRA, ALZ, CUE) and for forest (dark grey) and grassland (pale grey) habitats.
841 Significantly different endemicity by sampling point (Wilcoxon tests $p < 0.05$) between
842 forest and grassland communities at each hierarchical level is indicated by asterisks in
843 panels G, H, I.

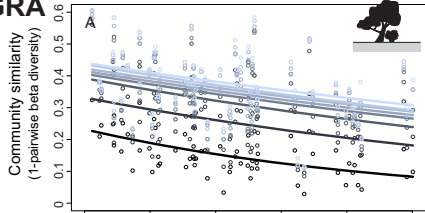




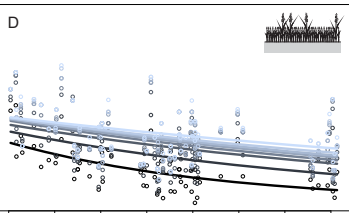
GRA*haplotypes**3% lineages***ALZ****CUE**

FOREST

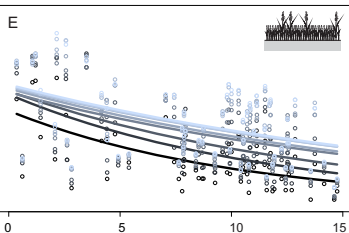
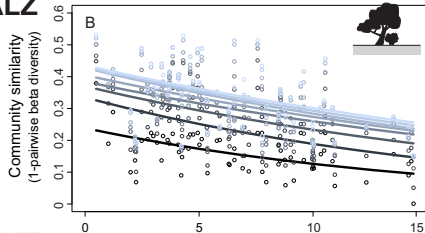
GRA



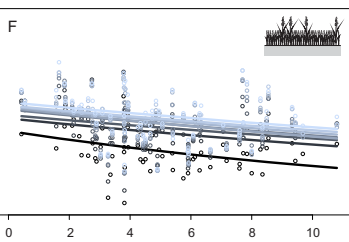
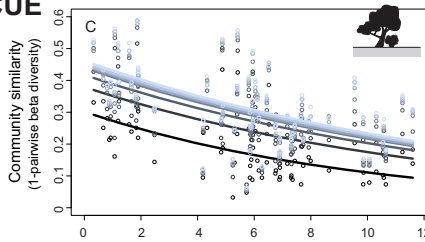
GRASSLAND



ALZ

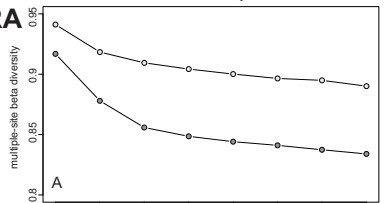


CUE



Local scale dissimilarity of communities

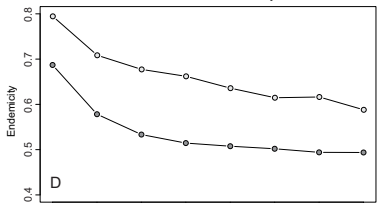
GRA



A

haplotypes 1% lineages 2% lineages 3% lineages 4% lineages 5% lineages 6% lineages 8% lineages

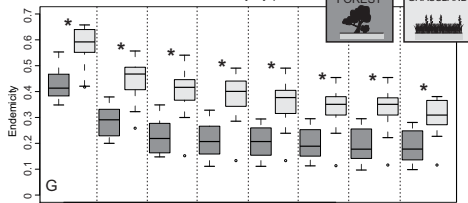
Local scale endemicity



D

haplotypes 1% lineages 2% lineages 3% lineages 4% lineages 5% lineages 6% lineages 8% lineages

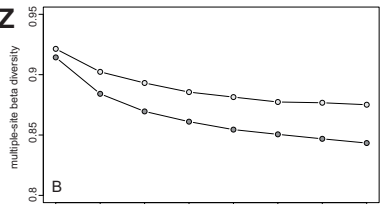
Endemicity by point



G

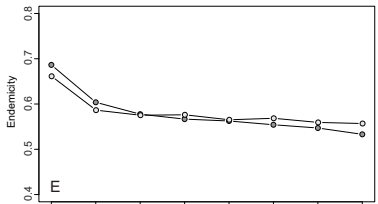
haplotypes 1% lineages 2% lineages 3% lineages 4% lineages 5% lineages 6% lineages 8% lineages

ALZ



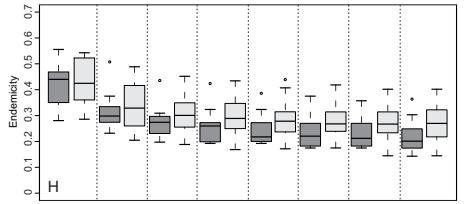
B

haplotypes 1% lineages 2% lineages 3% lineages 4% lineages 5% lineages 6% lineages 8% lineages



E

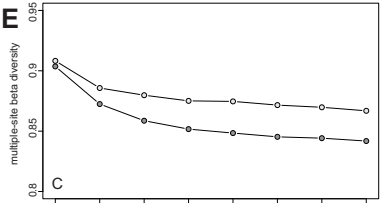
haplotypes 1% lineages 2% lineages 3% lineages 4% lineages 5% lineages 6% lineages 8% lineages



H

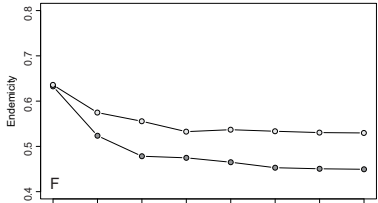
haplotypes 1% lineages 2% lineages 3% lineages 4% lineages 5% lineages 6% lineages 8% lineages

CUE



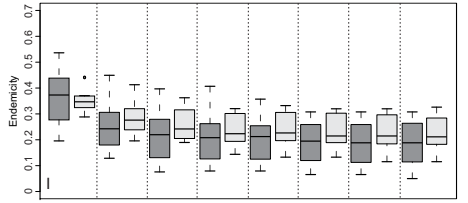
C

haplotypes 1% lineages 2% lineages 3% lineages 4% lineages 5% lineages 6% lineages 8% lineages



F

haplotypes 1% lineages 2% lineages 3% lineages 4% lineages 5% lineages 6% lineages 8% lineages



I

haplotypes 1% lineages 2% lineages 3% lineages 4% lineages 5% lineages 6% lineages 8% lineages

